

3-1-2020

Dosimetric Evaluation of PSMA PET-Delineated Dominant Intraprostatic Lesion Simultaneous Infield Boosts

Christopher D. Goodman
London Regional Cancer Program

Hatim Fakir
London Regional Cancer Program

Stephen Pautler
The University of Western Ontario

Joseph Chin
The University of Western Ontario

Glenn S. Bauman
London Regional Cancer Program, glenn.bauman@lhsc.on.ca

Follow this and additional works at: <https://ir.lib.uwo.ca/biophysicspub>

Citation of this paper:

Goodman, Christopher D.; Fakir, Hatim; Pautler, Stephen; Chin, Joseph; and Bauman, Glenn S., "Dosimetric Evaluation of PSMA PET-Delineated Dominant Intraprostatic Lesion Simultaneous Infield Boosts" (2020). *Medical Biophysics Publications*. 482.
<https://ir.lib.uwo.ca/biophysicspub/482>

Scientific Article

Dosimetric Evaluation of PSMA PET-Delineated Dominant Intraprostatic Lesion Simultaneous Infield Boosts



Christopher D. Goodman, MD,^a Hatim Fakir, PhD,^a Stephen Pautler, MD,^b Joseph Chin, MD,^b and Glenn S. Bauman, MD^{a,*}

^aDepartment of Radiation Oncology, London Regional Cancer Program, London, Ontario, Canada; and ^bDivision of Urology, Department of Surgery and Division of Surgical Oncology, Department of Oncology, Western University, London, Ontario, Canada

Received 11 April 2019; revised 30 August 2019; accepted 18 September 2019

Abstract

Purpose: Prostate cancer is multifocal. However, there often exists a single dominant focus in the gland responsible for driving the biology of the disease. Dose escalation to the dominant lesion is a proposed strategy to increase tumor control. We applied radiobiological modeling to evaluate the dosimetric feasibility and benefit of dominant intraprostatic lesion simultaneous in-field boosts (DIL-SIB) to the gross tumor volume (GTV), defined using a novel molecular positron emission tomography (PET) probe (18F-DCFPyL) directed against prostate specific membrane antigen (PSMA).

Methods and Materials: Patients with clinically localized, biopsy-proven prostate cancer underwent preoperative [¹⁸F]-DCFPyL PET/computed tomography (CT). DIL-SIB plans were generated by importing the PET/CT into the RayStation treatment planning system. GTV-PET for the DIL-SIB was defined by the highest %SUVmax (percentage of maximum standardized uptake value) that generated a biologically plausible volume. Volumetric arc-based plans incorporating prostate plus DIL-SIB treatment were generated. Tumor control probability (TCP) and normal tissue complication probability (NTCP) with fractionation schemes and boost doses specified in the FLAME (Investigate the Benefit of a Focal Lesion Ablative Microboost in Prostate Cancer; NCT01168479), PROFIT (Prostate Fractionated Irradiation Trial; NCT00304759), PACE (Prostate Advances in Comparative Evidence; NCT01584258), and hypoFLAME (Hypofractionated Focal Lesion Ablative Microboost in prostate Cancer 2.0; NCT02853110) protocols were compared.

Results: Comparative DIL-SIB plans for 6 men were generated from preoperative [¹⁸F]-DCFPyL PET/CT. Median boost GTV volume was 1.015 cm³ (0.42-1.83 cm³). Median minimum (D99%) DIL-SIB dose for F35_{BS}, F20_{BS}, F5_{BS}, and F5_{BSh} were 97.3 Gy, 80.8 Gy, 46.5 Gy, and 51.5Gy. TCP within the GTV ranged from 84% to 88% for the standard plan and 95% to 96% for the DIL-SIB plans. Within the rest of the prostate, TCP ranged from 89% to 91% for the standard plans and 90% to 92% for the DIL-SIB plans. NTCP for the rectum NTCP was similar for the DIL-SIB plans (0.3%-2.7%) compared with standard plans (0.7%-2.6%). Overall, DIL-SIB plans yielded higher uncomplicated TCP (NTCP, 90%-94%) versus standard plans (NTCP, 83%-85%).

Conclusions: PSMA PET provides a novel approach to define GTV for SIB-DIL dose escalation. Work is ongoing to validate PSMA PET-delineated GTV through correlation to coregistered postprostatectomy digitized histopathology.

© 2019 The Author(s). Published by Elsevier Inc. on behalf of American Society for Radiation Oncology. This is an open access article under the CC BY-NC-ND license (<http://creativecommons.org/licenses/by-nc-nd/4.0/>).

Sources of support: This work had no specific funding.

Disclosures: none.

* Corresponding author: Glenn S. Bauman, MD; E-mail: Glenn.bauman@lhsc.on.ca

<https://doi.org/10.1016/j.adro.2019.09.004>

2452-1094/© 2019 The Author(s). Published by Elsevier Inc. on behalf of American Society for Radiation Oncology. This is an open access article under the CC BY-NC-ND license (<http://creativecommons.org/licenses/by-nc-nd/4.0/>).

Introduction

Prostate cancer (PCa) is a multifocal disease. Histologic studies have reported that large prostate tumors are frequently accompanied by small, well-differentiated secondary tumors.¹ Accordingly, external beam radiation therapy (EBRT) for PCa has typically delivered a uniform dose to the entire gland. Dose escalation is correlated with a reduced risk of biochemical failure (BF) in the range of 1.8% per gray increase.² Whole-prostate dose escalation is possible to doses ≤ 86 Gy, above which bladder and rectal toxicity becomes intolerable.³ Unfortunately, locally recurrent disease is possible at this dose, suggesting that further escalation is required to obtain local tumor control.^{4,5}

Whole-mount pathology and genomic studies support the concept of a dominant intraprostatic lesion (DIL), wherein the largest or most aggressive intraprostatic lesion is responsible for driving the biology of the disease and thus prognosis.^{6,7} Up to one-third of patients treated with radical-intent EBRT for PCa will develop local recurrence, with the DIL being the most common site of recurrence.^{8,9} In the metastatic setting, Haffner et al¹⁰ tracked the clonal origin in a patient who died of metastases from PCa and proved that all metastases arose from a single prostatic lesion. Targeting the DIL with a boost dose is considered an effective strategy for dose escalation (and thus improved disease control) while respecting organ-at-risk (OAR) constraints. Indeed, it has been reported that dose distribution to the DIL is an independent risk factor for BF after primary EBRT in patients with PCa.¹¹

In a recent meta-analysis, von Eyben et al⁹ concluded that a boost to the DIL was effective and safe. Because the DIL constitutes a small portion of the prostate, ultrahigh boost doses to ≥ 90 Gy were feasible and appeared to be associated with improved outcomes. One study, included in their meta-analysis, reported a 10-year disease-free survival rate of 98% with boost to the DIL.

A systematic review of the literature by Bauman et al¹² demonstrated a large cohort of patients who have been treated for PCa with the addition of boosts to imaging-defined DILs. They note that there is a lack of standardized, reproducible, and accurate intraprostatic gross tumor volume (GTV) delineation guidelines. Various technologies for image guided definition of a DIL have been trialed, including contrast-enhanced magnetic resonance imaging (MRI), magnetic resonance spectroscopy, single-photon emission computerized tomography (SPECT), and positron emission tomography (PET)/computed tomography (CT). PET/CT using radiotracers directed against prostate-specific

membrane antigen (PSMA; a type II transmembrane protein encoded by the FOLH1 gene exhibiting 100- to 1000-fold overexpression in PCa¹³) has been shown to outperform multiparametric MRI when correlated with histology after prostatectomy.¹⁴⁻¹⁶

The aim of our study was to investigate the dosimetric feasibility and predicted biological efficacy of simultaneous in-field boost (SIB) to the DIL using PSMA PET–delineated GTVs in patients with primary PCa where the DIL is defined pathologically after radical prostatectomy. Plan comparisons were made using conventional (1.8-2.0 Gy/d) fractionation, moderate hypofractionation (2.5-3.0 Gy/d), and extreme hypofractionation (7-8 Gy/d).

Methods and Materials

Patient selection and PET/CT imaging

As part of a prospective clinical trial, IGPC-2 (Multi-modality Prostate Cancer Image Guided Interventions), patients with clinically localized, biopsy-proven PCa underwent preoperative [¹⁸F]-DCFPyL PET/CT. Inclusion criteria were biopsy-proven prostate adenocarcinoma and planned prostatectomy; exclusion criteria included prior treatment with hormones or radiation. All men were imaged at least 6 weeks after biopsy and within the 6 weeks before surgery. The multimodal imaging panel included dynamic contrast-enhanced CT (standard 3 mm CT slice thickness; Discovery VCT, GE Healthcare, Milwaukee, WI) to measure intraprostatic blood flow and develop quantitative maps of [¹⁸F]-DCFPyL uptake, PET/CT (GE Healthcare), and PET/MRI (Siemens BIOGRAPH mMR, Erlangen, Germany).

Structure delineation

To facilitate treatment planning, all CT and PET/CT images were transferred to RayStation V6.1 (RaySearch Inc.). The contouring of the prostate, bladder, rectum, and femoral heads was performed by a radiation oncologist based on the recommendations of the Radiation Therapy Oncology Group.¹⁷ The clinical target volume (CTV) included the prostate and proximal seminal vesicles. The planning target volume (PTV) was created by adding a uniform 5 mm margin to the CTV.¹⁸ The GTV based on the PSMA PET for the DIL-SIB was defined by the highest %SUVmax that generated a biologically plausible volume (GTV composed of contiguous voxels without gaps). The related PTV (PTV_{DIL}) was created by adding a uniform 5 mm margin to the GTV.

Simulated treatment planning

Standard plans aiming to treat the entire CTV are labeled *ST*, and plans including a boost to the DIL volume are termed *BS*. Three fractionations—77 Gy in 35 fractions, 60 Gy in 20 fractions, and 35 Gy in 5 fractions—were considered for the standard plans (Table 1) and are labeled F35_{ST}, F20_{ST}, and F5_{ST}, respectively. The prescriptions represent conventional, moderate, and extreme hypofractionations. Treatment plans were produced for each standard fractionation using dose objectives and constraints from the FLAME,¹⁹ PROFIT,²⁰ and PACE²¹ trials, respectively. The boost plan F35_{BS} was based on the FLAME trial. The prescriptions for boost plans F20_{BS} and F5_{BS} were set to ensure a biological effective dose equivalent to the F35_{BS} protocol (assuming an α/β ratio of 3 and no repopulation). An additional 5-fraction boost prescription of 50 Gy, F5_{B_{SH}}, was incorporated to investigate the more contemporary Hypo-FLAME trial (NCT02853110). The target coverage and OAR constraints are given in Table E2 (available online at <https://doi.org/10.1016/j.adro.2019.09.004>). All plans were generated with the RayStation treatment planning system, produced using volumetric modulated arc therapy. The RayStation biology module was used to calculate tumor control probability (TCP) and normal tissue complication probability (NTCP) values. For detailed information regarding these calculations please refer to the radiobiology modeling and evaluation section of the [Supplementary Materials](https://doi.org/10.1016/j.adro.2019.09.004) (available online at <https://doi.org/10.1016/j.adro.2019.09.004>).

Statistical analysis

Median values and ranges were calculated for the resulting dose-volume histogram (DVH) parameters, TCP and NTCP. The parameters for the standard and boost plans were compared using Wilcoxon signed-rank test using Origin (OriginLab). The 2 distributions were considered significantly different if the *P* values were less than .05.

Results

Six patients underwent preoperative PSMA PET/CT imaging (patients 1–6). Using National Comprehensive Cancer Network criteria, 2 patients were high risk and 4 were intermediate risk. Standard whole-prostate and OAR contours were created. DIL (GTV-PET) volumes were delineated for boost using an average %SUV_{max} of 30% (23%–40%). Median boost volumes were 1.015 cm³ (0.42–1.83 cm³). One patient (patient 5) had 2 separate GTV-PET volumes. The volumes, positions,

Table 1 Standard dose prescriptions to the PTV and total dose prescription to the PTV_{DIL} including the simultaneous integrated boost

Protocol	PTV	PTV _{DIL}	BED _{ST} (Gy ₃)	BED _{BS} (Gy ₃)
F35 _{ST}	77 Gy / 35	—	133.5	—
F35 _{BS}	77 Gy / 35	95 Gy / 35	133.5	181
F20 _{ST}	60 Gy / 20	—	120	—
F20 _{BS}	60 Gy / 20	79 Gy / 20	120	183
F5 _{ST}	35 Gy / 5	—	116.7	—
F5 _{BS}	35 Gy / 5	45.5 Gy / 5	116.7	183.5
F5 _{B_{SH}}	35 Gy / 5	50 Gy / 5	116.7	216.7

Abbreviations: BED = biologically equivalent dose; BS = boost plan; DIL = dominant intraprostatic lesion; PTV = planning target volume; ST = standard plan.

The related EQD2 and BED are calculated assuming an α/β equal to 3 and no repopulation.

and distances from the rectum are given in Table E4 (available online at <https://doi.org/10.1016/j.adro.2019.09.004>).

Comparative plans were generated for 6 patients using the prior specified fractionation schedules. The planning objectives and OAR dose constraints were met by all standard plans and by the boost plans for patients 2, 4, 5, and 6. Patients 1 and 3 had DIL volumes in close proximity to the rectum (0.2 mm and 3 mm, respectively), and rectal dose constraints for boost plans could not be achieved. In these cases, the dose constraints were met when prescribing the dose to a modified PTV_{DIL} (modPTV_{DIL}), defined as the PTV_{DIL} 5 mm away from the rectum. Despite the reduced PTV_{DIL} margins, GTV coverage (99% of the GTV covered by the boost prescription dose) was maintained for all cases and all boost protocols except the most hypofractionated schedule (F5_{B_{SH}}). Increasing the boost dose from 45.5 Gy (F5_{BS}) to 50 Gy (F5_{B_{SH}}) was achievable without exceeding the rectal dose constraints, except for patients 1 and 3. An example of dose distribution and the related DVH for patient 4 is shown in Figure 1. For all patients and dose fractionations, the dose distributions around the rectum and bladder and the corresponding DVHs display similar doses for both standard and boost plans. The isodose lines higher than 50% of the prescribed dose were prioritized to be similar between standard and boost protocols as the risks of rectal toxicity are thought to have a dose-response relationship in the intermediate- and high-dose volumes.

The median dose to 99% of the GTV (D_{99%}) in the standard plans was 77 Gy, 61 Gy, and 36 Gy for F35_{ST}, F20_{ST}, and F5_{ST}, respectively. The D_{99%} to GTV for the corresponding boost plans was 97 Gy, 81 Gy, and 47

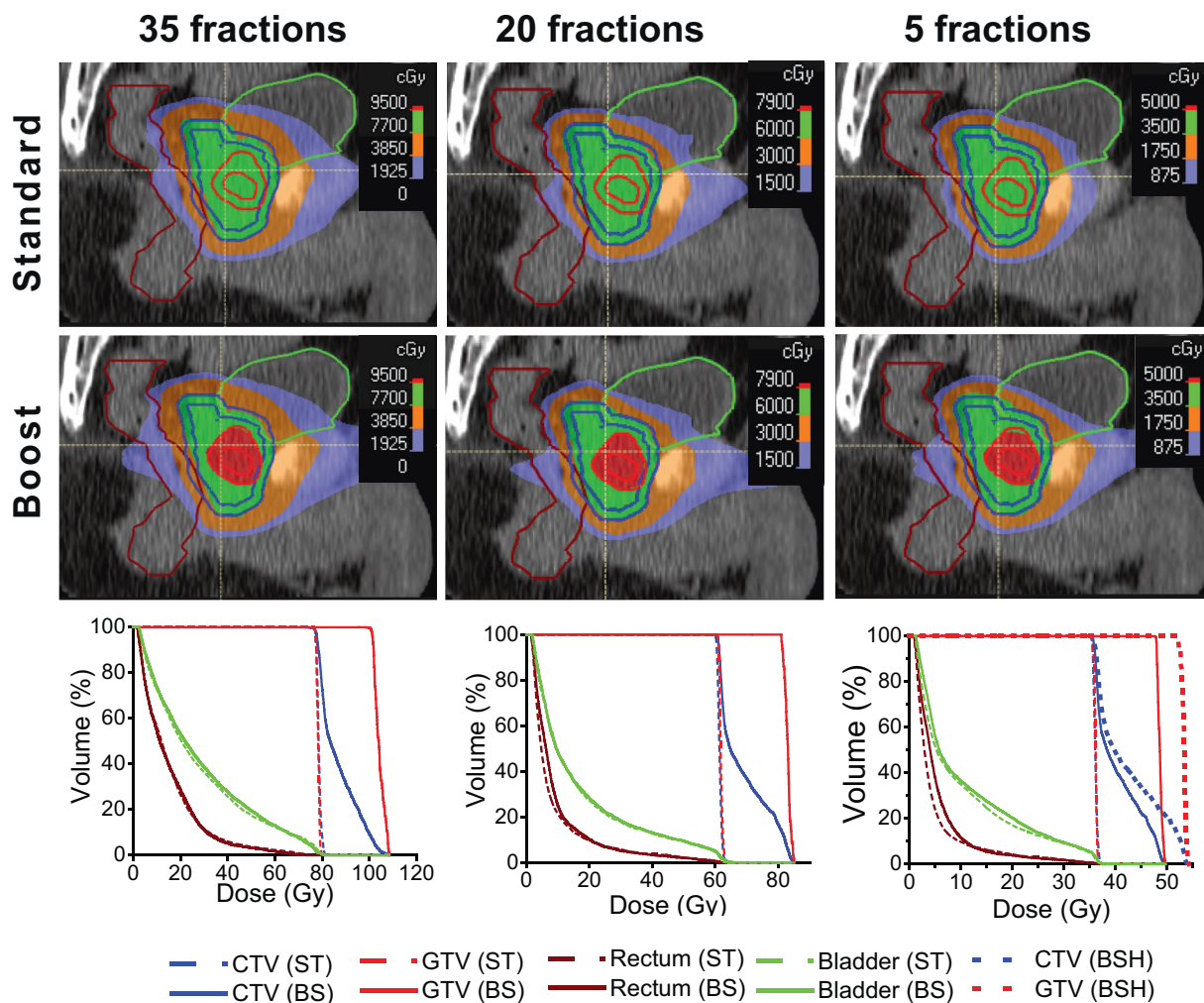


Figure 1 Dose distributions (sagittal projections) and corresponding DVHs for different fractionations for patient 4. The first and second rows represent standard and DIL boost plans, respectively. The third row contains comparative DVHs for the CTV, GTV, rectum, and bladder. The DVH for the 5 fractions regimen (F5_{BS}) includes the higher dose Hypo-FLAME (F5_{B_{SH}}) plan results as well (dotted lines). *Abbreviations:* CTV = clinical target volume; DIL = dominant intraprostatic lesion; DVH = dose-volume histogram; GTV = gross tumor volume; Hypo-FLAME = Hypofractionated Focal Lesion Ablative Microboost in prostatE Cancer 2.0.

Gy. The median D_{99%} for the 4 patients with F5_{B_{SH}} boost was 51 Gy. The boosts increased the mean dose to the GTV by 31%, 36%, 31%, and 48% for the F35_{BS}, F20_{BS}, F5_{BS}, and F5_{B_{SH}} protocols, respectively. The corresponding increase of the mean dose to the prostate excluding GTV (PROS-GTV) was 12%, 11%, 11%, and 14%. The differences in doses were statistically significant for both volumes ($P < .05$). The mean doses to the GTV and D_{1cc} to the rectum and bladder are shown in Table E5 (available online at <https://doi.org/10.1016/j.adro.2019.09.004>). The differences between standard and boost fractionations in rectum D_{1cc} were 3%, 5%, 6%, and 6%, and the differences in bladder D_{1cc} were 1%, 2%, 3%, and 3%. The physical DVH parameters for rectum and bladder were also compared for V_{50Gy} and V_{70Gy}; no differences were statistically significant ($P > .05$).

DVHs in equivalent 2 Gy per fraction doses (EQD₂) were generated to compare the biological effectiveness of the different fractionation schemes. DVHs for GTV, PROS-GTV, rectum, and bladder are shown in Figure 2. As prescriptions were adapted to be radiobiologically similar, boost dose DVHs are similar between protocols. The tails observed in the PROS-GTV DVH represent the dose fall-off outside the boost region. Figures E4, E5, and E6 (available online at <https://doi.org/10.1016/j.adro.2019.09.004>) show the comparison of the EQD₂ DVHs for the GTV, rectum, and bladder for each patient.

Figure 2 illustrates the significant increase in the GTV dose in the boost plans. EQD₂ mean doses to the GTV and PROS-GTV and D_{1cc}, V_{50Gy}, and V_{70Gy} to both rectum and bladder can be found in Table E6 (available online at <https://doi.org/10.1016/j.adro.2019.09.004>).

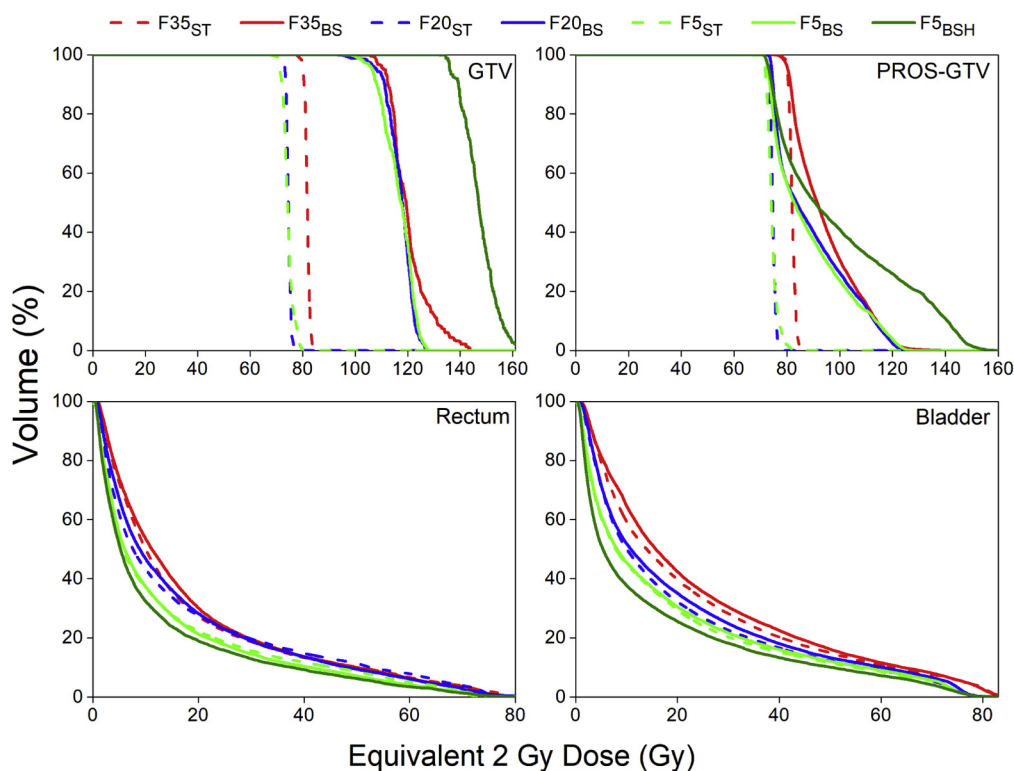


Figure 2 Average EQD_{2Gy} dose-volume histogram of the GTV, PROS-GTV, rectum, and bladder for all fractionations. *Abbreviations:* GTV = gross tumor volume; PROS-GTV = prostate excluding GTV.

The boosts increased the EQD₂ to the GTV to approximately 120 Gy. The mean GTV dose for F5_{BSH} was approximately 143 Gy. The corresponding rectal and bladder DVHs were similar for both the standard and the boost plans.

Figure 3 displays TCP values for the GTV and PROS-GTV compared with NTCP for both rectum and bladder. The effectiveness of the treatment protocols is assessed using the complication factor $P+$, which represents the probability of tumor control without rectal complications. For the standard plans, the mean TCPs for the GTV were 87%, 84%, and 84% for F35_{ST}, F20_{ST}, and F5_{ST}. The boost increased the TCPs to approximately 94% for all 3 protocols. The corresponding mean TCP for F5_{BSH} was approximately 96%. The TCP for PROS-GTV was approximately 90% for the standard plans and 91% for the boost plans. The TCPs for PROS-GTV are higher than for the GTV because of the lower clonogenic cell density. The differences in NTCP between standard and boost plans were not significant. The mean probability of uncomplicated tumor control ($P+$) for the standard plans was 85%, 82%, and 83% for F35_{ST}, F20_{ST}, and F5_{ST}, respectively. The corresponding values for the boost plans (F35_{BS}, F20_{BS}, and F5_{BS}) were 92%, 92%, and 94%. The mean $P+$ for F5_{BSH} was 96%.

Discussion

In this study we applied radiobiological modeling to evaluate the dosimetric feasibility and biological effectiveness of DIL-SIB to GTVs defined using a novel molecular PET probe directed against PSMA. TCP and NTCP were calculated for 6 patients with prescriptions ranging from conventionally to extremely hypofractionated.

Optimal identification of the DIL is an area of ongoing discordance. In 2013, a systematic review by Bauman et al¹² identified 13 studies describing 11 unique patient series with a total of 833 patients receiving an imaging defined boost to the DIL. They noted significant heterogeneity in technique for delineating a boost volume. Techniques for delineation include single-parameter MRI, multiparameter MRI (mpMRI), SPECT, and PET. Data for SPECT are underwhelming, with 1 study noting no correlation between tracer uptake and presence of cancer on whole-mount pathology.²² MRI is regarded as the current gold standard for imaging delineation. The FLAME randomized trial used mpMRI for image delineation.¹⁹ Test performance (as measured by sensitivity/specificity or receiver operating characteristic analysis) is worst for single-sequence MRI with performance improving for multiparametric MRI, which is reflected in current consensus guidelines recommending T2W (T2

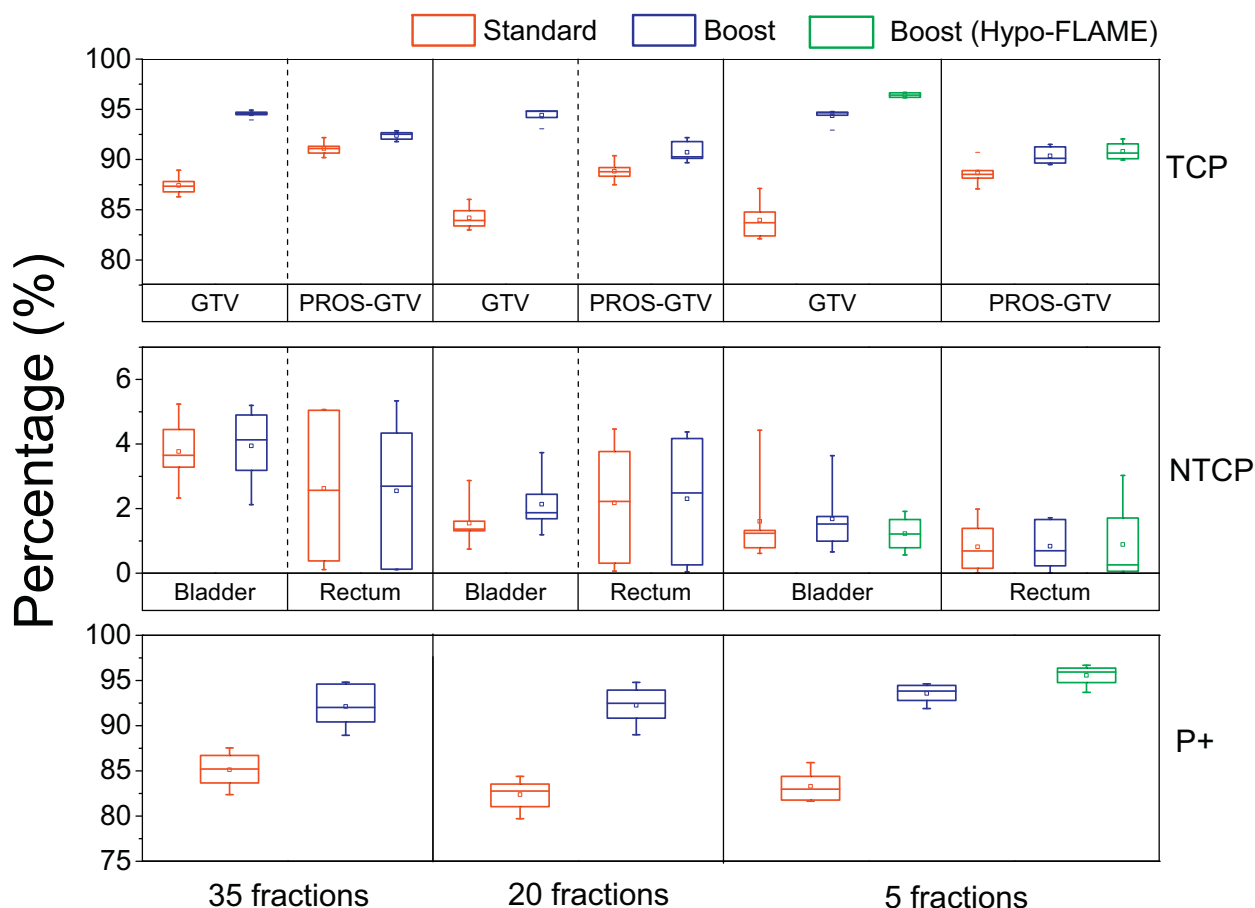


Figure 3 Tumor control probability (TCP) for the GTV and PROS-GTV, NTCP for bladder and rectum, and probability of uncomplicated tumor control ($P+$) relative to rectal toxicity. *Abbreviations:* GTV = gross tumor volume; PROS-GTV = prostate excluding GTV.

weighted) + DWI (diffusion-weighted magnetic resonance imaging) + DCE (dynamic contrast enhanced magnetic resonance imaging) for lesion detection.²³

Chan et al²⁴ examined the utility of choline PET compared with MRI for lesion delineation. They found that with shorter uptake times, choline PET resulted in a lower accuracy (61.6%) compared with T2W MRI (70.2%), but with a longer uptake time the accuracy of PET surpassed MRI. They additionally noted that PET/MRI together identified aggressive disease better than either modality alone.²⁴ In a recent study, Piert et al²⁵ compared the accuracy of mpMRI and choline PET for detecting clinically significant PCa. Ten patients underwent mpMRI and PET/CT before radical prostatectomy. Two radiologists independently determined tumor boundaries based on mpMRI, and PET/CT data were analyzed using a semiautomatic segmentation routine. The results were compared with histopathologic registrations, and all were found to grossly underestimate tumor volume. However, when the information was combined into a conglomerate volume, the percentage of

underestimated tumor volume improved significantly and the necessary safety margin needed to safely cover the entire tumor decreased from 11 to 15 mm to 9 mm.

There exists a reported correlation between PSMA ligand expression/uptake and Gleason score, d'Amico risk group, and features of tumor aggressiveness.²⁶ This suggests that PSMA PET may identify more clinically relevant lesions compared with choline PET/CT or mpMRI. Comparisons of PSMA PET/CT and mpMRI for DIL delineation against postprostatectomy histopathology have reported good sensitivity and specificity for both modalities. Multiple studies have reported that the highest degree of accuracy is achieved when combined PSMA PET/MRI data are employed for lesion delineation.¹⁴⁻¹⁶ This supports the growing consensus that a hybrid of mpMRI and PSMA PET data provides the most robust imaging-guided delineation of DIL volumes.

Kuang et al²⁷ used choline PET to derive boost volumes and compared 2 dose fractionations. Whole prostate PTV prescription was 79 Gy in both plans, with the second plan incorporating simultaneous boost doses of

100 Gy and 105 Gy to the IDL, defined by 60% and 70% of maximum prostatic uptake on 18F-choline PET, respectively. The boost plan was associated with significantly higher TCP compared with the nonboost plan at all 4 α/β ratios examined ($P < .001$). They noted a small but significant increase in NTCP for grade 2 late rectal toxicity (2.2% vs 2.8%, $P < .001$). There was no significant difference in bladder NTCP between the 2 plans.²⁷ In a similar study from Zamboglou et al²⁸ GTVs were generated on the basis of an intraprostatic uptake of ⁶⁸Ga-HBED-CC PSMA-PET. They used a threshold % SUVmax of 30% to define GTV-PET. Two intensity modulated radiation therapy plans were then generated for each patient, the first consisting of 77 Gy to the whole prostate and the second 77 Gy to the whole gland with simultaneous integrated boost to GTV-PET up to 95 Gy. Mean volume of generated GTV-PETs was 7.5 ± 4.8 mL. TCP-PET was found to be significantly higher for plan⁹⁵ (100% vs 55%, $P < .0001$). No significant differences in rectal or bladder NTCPs were observed between the 2 plans.²⁸

Our study examined a variety of fractionation schedules to simulate the effects on TCP and NTCP of a boost to a DIL defined by PSMA PET uptake. With consideration for delineating a biologically plausible volume, we used a range of 23% to 40% SUVmax for definition of GTV-PET (mean threshold SUVmax of 30%). Median GTV-PET volume was 1.0 cm^3 ($0.4\text{--}1.8 \text{ cm}^3$). Dose objectives and constraints were met for all plans except 2 of the higher dose (50 Gy) 5-fraction boost protocol (F5_{B5H}).

GTV-PET volume was not a limiting factor to boost dose escalation. Instead, we encountered a more significant effect with the location of the GTV-PET volume in relation to surrounding OARs. Proximity of the DIL to the rectum was the primary dose-limiting factor. For such cases, to meet rectal constraints, we used a modified PTV that is 5 mm away from the rectal wall. Despite these modifications, GTV coverage of at least 99% of the prescription boost dose was achieved for nearly all plans. In patients 1 and 3, the proximity of the DIL to the rectum precluded a F5_{B5H} boost without exceeding rectal constraints. For all cases, the rectum and bladder doses were generally lower in 5-fraction plans, mainly owing to stricter planning constraints. We found a 7% to 10% increase in TCP within the boost plans, which was statistically significant compared with standard plans. NTCP values were not statistically significantly different between standard and boost plans.

Our results compare favorably to the previously cited studies, showing a significant increase in TCP with DIL boost compared with standard plans with no significant difference in NTCP. We recognize several limitations with this work. Primarily, our study is limited by a small sample size. The cases presented herein are representative of typical DIL volumes and locations within the prostate

gland and offered sufficient data to discuss the proposed dose escalation methodologies and compare different fractionation schedules within the confines of this feasibility study. In the future we hope to leverage increasing access to PSMA PET to design larger-scale studies and enable a more robust analysis. Our study also lacks pathologic validation of our PSMA PET-derived volumes. All patients underwent radical prostatectomy as part of their definitive treatment, and work is ongoing to complete coregistration of applicable histopathology to PSMA PET data. Additionally, our model does not account for intrafraction sources of error.

There is mounting evidence to suggest that a boost to an imaging-defined DIL would lead to improved outcomes with minimal to negligible effects on toxicity rates. To employ this technique clinically, more work is required to standardize and validate a technique for DIL definition. Several large clinical trials are actively investigating the use of DIL boost to improve outcomes. The previously cited FLAME randomized trial, with a target accrual of 571 participants, is powered to detect a 10% improvement in 5-year freedom from BF. Initial reports suggest that at a median follow-up of 55 months there are no significant differences in toxicity rates between standard and boost arms. Forthcoming results from this and similar trials will provide much-needed guidance on the delineation of boost GTVs and the efficacy of DIL boost. Although the FLAME protocol used mpMRI, the described workflow and dose constraints could be readily adapted for PSMA-PET based GTV delineation.

An additional boundary to clinical deployment is the necessity for robust motion management to ensure proper delivery of boost dose to the specified volume. Because of the high dose gradients, risk of toxicity, and the required geometric precision in DIL-boost treatments, assessment of various sources of uncertainty and mitigation strategies is warranted. First, the uncertainties in GTV contouring may require adding large margins that would ultimately lead to higher doses to the surrounding tissue. However, we have recently demonstrated that mpMRI and PET may enable more accurate GTV delineation, allowing smaller margins and better dose sparing.^{13,29}

Interfraction variations are now routinely and effectively reduced by controlling rectum and bladder volumes³⁰ in conjunction with proper in-room image guidance (usually daily cone beam CT for linear accelerator-based treatments). Furthermore, most DIL boost and hypofractionation studies such as FLAME and Hypo-FLAME require intraprostatic fiducial markers to improve prostate localization.¹⁹

Intrafraction organ motion warrants special attention in high-precision DIL-boost treatments compared with more conventionally fractionated schedules. In a previous experimental investigation, we showed that DIL boosts can be safely achieved in the presence of intrafraction

motion when using a PTV margin of 7 mm.³¹ More recent studies have shown that tracking intraprostatic fiducial markers and accounting for 6 degrees of freedom in prostate motion can reliably monitor prostate position during delivery with an accuracy of $0.2^\circ \pm 1.3^\circ$ and 0.1 ± 0.5 mm for rotation and translation, respectively.³² Fiducial tracking has been associated with lower toxicity.³⁰ Faster delivery (approximately 1 minute) using flattening filter free mode has been shown to further reduce the effects of intrafraction motion.³³

In our institution, all patients undergo rectum and bladder preparation, and fiducial markers are implanted for all extreme hypofractionation cases. Cone beam CT and 6 degrees of freedom couch are used for the initial treatment setup, and triggered kV imaging is used for prostate tracking as a quality assurance during treatment within a 3 mm margin. All cases are planned with volume modulated arc therapy and flattening filter free beams. Based on the published evidence, we believe this process offers safer and more reliable delivery of DIL-boost treatments.

Conclusions

It is both feasible and safe to construct radiobiologically equivalent plans for a variety of dose fractionations to deliver a boost to the DIL while meeting OAR constraints. The boost dose is limited by lesion size and proximity to OARs, with less effect of fractionation approach. Further study and better understanding of the interplay among lesion morphology, anatomic factors, and dosimetry are required.

Supplementary data

Supplementary material for this article can be found at <https://doi.org/10.1016/j.adro.2019.09.004>

References

- Cooper CS, Eeles R, Wedge DC, et al. Analysis of the genetic phylogeny of multifocal prostate cancer identifies multiple independent clonal expansions in neoplastic and morphologically normal prostate tissue. *Nat Genet.* 2015;47:367-372.
- Viani GA, Stefano EJ, Afonso SL. Higher-than-conventional radiation doses in localized prostate cancer treatment: A meta-analysis of randomized, controlled trials. *Int J Radiat Oncol Biol Phys.* 2009;74:1405-1418.
- Spratt DE, Zumsteg ZS, Ghadjar P, et al. Comparison of high-dose (86.4 Gy) IMRT vs combined brachytherapy plus IMRT for intermediate-risk prostate cancer. *BJU Int.* 2014;114:360-367.
- Cellini N, Morganti AG, Mattiucci GC, et al. Analysis of intraprostatic failures in patients treated with hormonal therapy and radiotherapy: Implications for conformal therapy planning. *Int J Radiat Oncol Biol Phys.* 2002;53:595-599.

- Martinez AA, Gonzalez J, Ye H, et al. Dose escalation improves cancer-related events at 10 years for intermediate- and high-risk prostate cancer patients treated with hypofractionated high-dose-rate boost and external beam radiotherapy. *Int J Radiat Oncol Biol Phys.* 2011;79:363-370.
- Mouraviev V, Villers A, Bostwick DG, et al. Understanding the pathological features of focality, grade and tumour volume of early-stage prostate cancer as a foundation for parenchyma-sparing prostate cancer therapies: Active surveillance and focal targeted therapy. *BJU Int.* 2011;108:1074-1085.
- Pucar D, Hricak H, Shukla-Dave A, et al. {A figure is presented} Clinically significant prostate cancer local recurrence after radiation therapy occurs at the site of primary tumor: Magnetic resonance imaging and step-section pathology evidence. *Int J Radiat Oncol Biol Phys.* 2007;69:62-69.
- Arrayeh E, Westphalen AC, Kurhanewicz J, et al. Does local recurrence of prostate cancer after radiation therapy occur at the site of primary tumor? Results of a longitudinal MRI and MRSI study. *Int J Radiat Oncol Biol Phys.* 2012;82:e787-e793.
- Von Eyben FE, Kiljunen T, Kangasmaki A, et al. Radiotherapy boost for the dominant intraprostatic cancer lesion - a systematic review and meta-analysis. *Clin Genitourin Cancer.* 2016;14:189-197.
- Haffner MC, Mosbrugger T, Esopi DM, et al. Tracking the clonal origin of lethal prostate cancer. *J Clin Invest.* 2013;123:4918-4922.
- Zamboglou C, Klein CM, Thomann B, et al. The dose distribution in dominant intraprostatic tumour lesions defined by multiparametric MRI and PSMA PET/CT correlates with the outcome in patients treated with primary radiation therapy for prostate cancer. *Radiat Oncol.* 2018;13:1-8.
- Bauman G, Haider M, Van Der Heide UA, et al. Boosting imaging defined dominant prostatic tumors: A systematic review. *Radiother Oncol.* 2013;107:274-281.
- Bauman G, Martin P, Thiessen JD, et al. [18F]-DCFPyL positron emission tomography/magnetic resonance imaging for localization of dominant intraprostatic foci: First experience. *Eur Urol Focus.* 2016;4:5-9.
- Rhee H, Thomas P, Shepherd B, et al. Prostate specific membrane antigen positron emission tomography may improve the diagnostic accuracy of multiparametric magnetic resonance imaging in localized prostate cancer. *J Urol.* 2016;196:1261-1267.
- Eiber M, Weirich G, Holzapfel K, et al. Simultaneous 68Ga-PSMA HBED-CC PET/MRI improves the localization of primary prostate cancer. *Eur Urol.* 2016;70:829-836.
- Zamboglou C, Drendel V, Jilg CA, et al. Comparison of 68Ga-HBED-CC PSMA-PET/CT and multiparametric MRI for gross tumour volume detection in patients with primary prostate cancer based on slice by slice comparison with histopathology. *Theranostics.* 2017;7:228-237.
- Parliament M, Winter K, Seider M, et al. Effect of standard vs dose-escalated radiation therapy for patients with intermediate-risk prostate cancer. *JAMA Oncol.* 2018;4:e180039.
- Oehler C, Lang S, Dimmerling P, et al. PTV margin definition in hypofractionated IGRT of localized prostate cancer using cone beam CT and orthogonal image pairs with fiducial markers. *Radiat Oncol.* 2014;9:229.
- Lips IM, van der Heide UA, Haustermans K, et al. Single blind randomized phase III trial to investigate the benefit of a focal lesion ablative microboost in prostate cancer (FLAME-trial): Study protocol for a randomized controlled trial. *Trials.* 2011; 12:255.
- Catton CN, Lukka H, Gu C-S, et al. Randomized trial of a hypofractionated radiation regimen for the treatment of localized prostate cancer. *J Clin Oncol.* 2017;35:1884-1890.

21. Morrison K, Tree A, Khoo V, et al. The PACE trial: International randomised study of laparoscopic prostatectomy vs. stereotactic body radiotherapy (SBRT) and standard radiotherapy vs. SBRT for early stage organ-confined prostate cancer. *J Clin Oncol*. 2018; 36(6_suppl):TPS153.
22. Mouraviev V, Madden JF, Broadwater G, et al. Use of ¹¹¹In-capromab pendetide immunoscintigraphy to image localized prostate cancer foci within the prostate gland. *J Urol*. 2009;182:938-948.
23. Barentsz JO, Richenberg J, Clements R, et al. ESUR prostate MR guidelines 2012. *Eur Radiol*. 2012;22:746-757.
24. Chan J, Syndikus I, Mahmood S, et al. Is choline PET useful for identifying intraprostatic tumour lesions? A literature review. *Nucl Med Commun*. 2015;36:871-880.
25. Piert M, Shankar PR, Montgomery J, et al. Accuracy of tumor segmentation from multi-parametric prostate MRI and ¹⁸F-choline PET/CT for focal prostate cancer therapy applications. *EJNMMI Res*. 2018;8:1-14.
26. Koerber SA, Utzinger MT, Kratochwil C, et al. ⁶⁸Ga-PSMA11-PET/CT in newly diagnosed carcinoma of the prostate: correlation of intraprostatic PSMA uptake with several clinical parameters. *J Nucl Med*. 2017;58:1943-1948.
27. Kuang Y, Wu L, Hirata E, et al. Volumetric modulated arc therapy planning for primary prostate cancer with selective intraprostatic boost determined by ¹⁸F-choline pet/ct. *Int J Radiat Oncol Biol Phys*. 2015;91:1017-1025.
28. Zamboglou C, Sachpazidis I, Koubar K, et al. Evaluation of intensity modulated radiation therapy dose painting for localized prostate cancer using ⁶⁸Ga-HBED-CC PSMA-PET/CT: A planning study based on histopathology reference. *Radiother Oncol*. 2017; 123:472-477.
29. Gibson E, Bauman GS, Romagnoli C, et al. Toward prostate cancer contouring guidelines on magnetic resonance imaging: Dominant lesion gross and clinical target volume coverage via accurate histology fusion. *Int J Radiat Oncol Biol Phys*. 2016;96:188-196.
30. Clemente S, Nigro R, Oliviero C, et al. Role of the technical aspects of hypofractionated radiation therapy treatment of prostate cancer: A review. *Int J Radiat Oncol Biol Phys*. 2015;91:182-195.
31. Abdellatif A, Craig J, Jensen M, et al. Experimental assessments of intrafractional prostate motion on sequential and simultaneous boost to a dominant intraprostatic lesion. *Med Phys*. 2012;39:1505-1517.
32. Kim J-H, Nguyen DT, Booth JT, et al. The accuracy and precision of kilovoltage intrafraction monitoring (KIM) six degree-of-freedom prostate motion measurements during patient treatments. *Radiother Oncol*. 2018;126:236-243.
33. Benedek H, Lerner M, Nilsson P, et al. The effect of prostate motion during hypofractionated radiotherapy can be reduced by using flattening filter free beams. *Phys Imaging Radiat Oncol*. 2018;6:66-70.